

Sensitivity and specificity of atmospheric trace gas detection by proton-transfer-reaction mass spectrometry

Joost de Gouw^{a,b,*}, Carsten Warneke^c, Thomas Karl^d,
Gunter Eerdekens^c, Carina van der Veen^c, Ray Fall^{b,e}

^a NOAA Aeronomy Laboratory, 325 Broadway R/AL7, Boulder, CO, USA

^b Cooperative Institute for Research in Environmental Sciences, University of Colorado, Boulder, CO, USA

^c Institute for Marine and Atmospheric Research, Utrecht University, Utrecht, The Netherlands

^d National Center for Atmospheric Research, Boulder, CO, USA

^e Department of Chemistry and Biochemistry, University of Colorado, Boulder, CO, USA

Received 19 December 2001; accepted 24 May 2002

Abstract

Proton-transfer-reaction mass spectrometry (PTR–MS) has emerged as a useful tool to study the atmospheric chemistry of volatile organic compounds (VOCs), which are implicated in the formation of ozone and aerosols in polluted air. In PTR–MS, ambient air is continuously pumped through a drift-tube reactor and the VOCs in the sample are ionized using proton-transfer reactions with H_3O^+ ions. The H_3O^+ and product ions are detected with a quadrupole mass spectrometer. The technique combines a fast response time (1 s) with a low detection limit (10–100 parts-per-trillion), and allows atmospheric measurements of many important VOCs and their oxidation products in a variety of field experiments. Here, the sensitivity of PTR–MS with respect to a number of VOCs is characterized. The measured sensitivity, obtained using calibrated mixtures of VOCs in air, is compared with a calculated sensitivity and a reasonable agreement is obtained. It is shown how the sensitivity depends on the pressure in the drift tube and on the humidity of the sample air. In PTR–MS, only the mass of the ionized trace gases is determined, which is a useful but not a unique indicator of the trace gas identity. A combination of gas chromatography and PTR–MS (GC–PTR–MS) has been developed to investigate which compounds contribute to the signal at a certain mass. Air samples collected in the city of Utrecht in The Netherlands and at the remote Sonnblick Observatory in Austria were analyzed by GC–PTR–MS. The results clearly indicate that PTR–MS measurements of VOCs such as methanol, acetonitrile, acetaldehyde, benzene and toluene are free from interference by other compounds. For other VOCs, such as acetone and methyl ethyl ketone, interference cannot always be ruled out entirely. For some masses like 69 amu, a large number of biogenic VOCs produce the same signal, demonstrating the need for GC–PTR–MS methods. It is also shown that PTR–MS measurements can likely be used to determine the sum of the concentration of C_2 -benzenes, despite the fact that these compounds cannot be independently measured with PTR–MS. (Int J Mass Spectrom 223–224 (2003) 365–382)

© 2002 Elsevier Science B.V. All rights reserved.

Keywords: Volatile organic compounds; Proton-transfer-reaction mass spectrometry; Atmospheric trace gas

* Corresponding author. E-mail: jdegouw@al.noaa.gov

1. Introduction

Volatile organic compounds (VOCs) are released to the Earth's atmosphere from a wide variety of sources, both of natural and man-made origin [1]. Although some sources are reasonably well quantified, many uncertainties remain about the ultimate fate of these compounds in the atmosphere. Most VOCs react with hydroxyl radicals (OH); some can be photolyzed, react with ozone, or at night with nitrate radicals (NO_3). The products of the reactions may react further or may be lost from the atmosphere by deposition at the Earth's surface or through uptake by clouds and aerosols followed by rainout. The magnitude of the different loss processes is largely unknown, and hence the atmospheric budget of organic carbon remains very uncertain. Resolving the uncertainties is one of the important problems in our understanding of the chemistry of the lower atmosphere. The photo-oxidation of VOCs is implicated in the formation of ozone and aerosols in polluted air, which are both major air pollutants, have adverse health effects to humans, and are significant factors in the Earth's climate system [2].

Proton-transfer-reaction mass spectrometry (PTR-MS) is a recent technique for measuring trace amounts of VOCs in air, and was developed by Lindinger et al. [3] at the University of Innsbruck. In PTR-MS, air is continuously pumped through a reactor, and the VOCs are ionized by proton-transfer reactions with H_3O^+ ions. The H_3O^+ and product ions are extracted from the gas flow, and are mass analyzed and detected with a quadrupole mass spectrometer. PTR-MS is a well-suited tool for studying the atmospheric chemistry of organic compounds, because it allows many important VOCs from natural and man-made origin to be measured along with their oxidation products. Two features that set PTR-MS apart from its alternatives like GC-MS are (1) the fast time response of only seconds or less, and (2) the capability of performing stand-alone measurements over extended periods of time. The fast response allows applications in rapidly changing air masses, for instance when measuring from a fast moving platform such as an aircraft, when monitoring a compound with a very short lifetime,

or when measuring close to a source. The long-term measurement capability allows the monitoring of air masses from ground-based sites.

The basic concept of PTR-MS, chemical ionization of trace gases using a suitable ion-molecule reaction and detection with a mass spectrometer, has been used in many atmospheric measurements. Examples include measurements of nitric acid (HNO_3) [4,5]; sulfuric acid (H_2SO_4) [6]; hydroxyl radicals (OH) [7]; hydrogen cyanide (HCN) [8]; dimethyl sulfide (CH_3SCH_3) and its oxidation products [6,9]; and VOCs such as acetonitrile (CH_3CN) [8], acetone (CH_3COCH_3), formic (HCOOH) and acetic acid (CH_3COOH) [10]. A difference between PTR-MS and these other techniques is the use of a drift tube instead of a flow tube as the reactor. In a drift tube, an electric field is applied in the axial direction, which allows increasing the ion kinetic energy and thus reducing the clustering of the reagent and product ions with water. As a result, the ion chemistry involved in PTR-MS is greatly simplified, which facilitates the detection of many different compounds with the same setup. A disadvantage is the fact that the electric field limits the reaction time of the H_3O^+ ions and also the pressure in the drift tube. Therefore, the conversion efficiency of primary into product ions in PTR-MS is slightly smaller than for some of the alternatives.

Since 1998, PTR-MS has been used in a number of laboratory and field studies of the atmosphere. Onboard a Citation research aircraft, PTR-MS and other instruments were used to study the composition of the atmosphere over the tropical rain forest in Surinam [11–14], and the outflow of polluted air from India [15]. Ship-based measurements were carried out on the Indian Ocean by Lelieveld et al. [16] studying polluted air masses from India, and by Warneke and de Gouw looking at clean marine conditions [17]. Ground-based measurements were performed at the Sonnblick Observatory in the Austrian Alps [18,19]. Karl et al. [20] and more recently Rinne et al. [21] demonstrated the feasibility of using PTR-MS for eddy covariance measurements, in which concentrations are monitored simultaneously with the vertical wind speed in order to quantify the

surface–atmosphere exchange of trace compounds. Laboratory applications included emission studies of burning and smoldering biomass [22], wetted, dead plant matter [23] and wounded leaves [19,24]. de Gouw et al. [25,26] used a similarly designed instrument to study the emissions from drying hay crops.

The sensitivity of PTR–MS depends on numerous factors, including the conversion efficiency of the primary H_3O^+ into product ions [3]. Here, it is shown using measurements and calculations how the conversion efficiency depends on parameters such as the pressure and electric field. As mentioned above, clustering of H_3O^+ ions with water molecules is prevented in PTR–MS by the enhanced kinetic energy of the ions in the drift tube. Depending on the operating conditions, however, there can be a significant number of $\text{H}_3\text{O}^+(\text{H}_2\text{O})_n$ ions in the drift tube. As a result, the sensitivity can be dependent on the humidity of the sampled air as shown by Warneke et al. [27]. In this paper, we use a simple model to calculate the distribution of $\text{H}_3\text{O}^+(\text{H}_2\text{O})_n$ ions in the drift tube, which allows the sensitivity to be evaluated as a function of the humidity.

In PTR–MS, only the mass of the product ions is determined, which is a valuable but certainly not a unique indicator of the identity of trace gases. It is clear that different isomers cannot be separated in this manner. Moreover, the interpretation of the mass spectra can be complicated by the fragmentation of product ions, which may lead to mass overlap [13]. As a result of the recent PTR–MS work, a lot of information has become available regarding the specificity of PTR–MS detection of many trace gases. In this work, we expand that information by coupling a gas chromatographic column to a PTR–MS instrument, which allows the contributions from different compounds observed at a single mass to be separated. The GC–PTR–MS combination was introduced by Karl et al. [18] and is used here to analyze a number of air samples collected in the city of Utrecht in The Netherlands and on top of the Sonnblick in the Austrian Alps. From the results, a detailed insight is obtained into the specificity of PTR–MS measurements of many different trace gases.

2. Experimental setup

Lindinger et al. [3] have described the PTR–MS in detail, and therefore only a brief description is given here. The PTR–MS consists of (1) an ion source to produce H_3O^+ ions, (2) a drift tube where the proton-transfer reactions between H_3O^+ and the different trace gases take place, and (3) a quadrupole mass spectrometer to measure the reagent and product ions.

Ions are produced in a hollow-cathode discharge in water vapor, which forms an intense source of H_3O^+ ions: H_3O^+ count rates of over 4×10^6 counts s^{-1} are routinely observed with the mass spectrometer. A water vapor flow of $8 \text{ STP cm}^3 \text{ min}^{-1}$ (STP = standard temperature of 273.15 K and pressure of 1 atm) is pumped through the source; about 5% of this flow reaches the drift tube, leading to an increased humidity of the sampled air.

The drift tube consists of a $9.6 \text{ cm} \times 5.0 \text{ cm}$ i.d. tube made of electrically isolated stainless steel rings. The rings are connected with resistors, and a voltage of up to 600 V can be applied over the entire set of rings to setup a homogeneous electric field in the drift tube. The sample air is pumped at a flow of $\sim 30 \text{ STP cm}^3 \text{ min}^{-1}$ through the drift tube. The residence time of air in the drift tube is approximately 1 s, which is a limiting factor to the response time of the system. The sample air and a fraction of the ions exit the drift tube through an orifice and enter a small intermediate chamber, which is pumped by a turbo pump (Pfeiffer TPD 022). The intermediate chamber separates the pressure of 2–3 mbar in the drift tube from the high vacuum in the mass spectrometer chamber (10^{-5} mbar). In the intermediate chamber, ions are focused onto the opening of the quadrupole mass spectrometer (Balzers QMG422).

A schematic diagram of the gas inlet system used in Utrecht is shown in Fig. 1. A diaphragm pump is used to pump the gas inlet. A pressure controller regulates the inlet flow, such that the pressure upstream of the controller is kept at a constant value. In this way, the pressure in the drift tube of the PTR–MS is held constant, independent of the ambient pressure. With this setup the sample flow is only exposed to

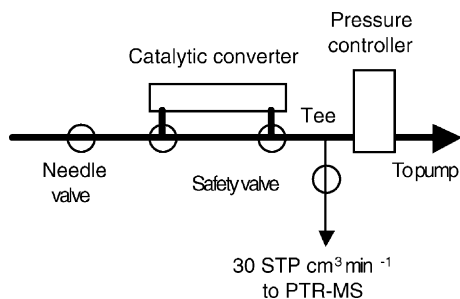


Fig. 1. Schematic diagram of the gas inlet system for the PTR-MS used in Utrecht.

Teflon parts, which is important to minimize memory effects and the build-up of impurities in the inlet system.

A problem when measuring small mixing ratios is a proper determination of the background impurities in the system, which vary from a few to a few hundred pptv in the PTR-MS, depending on the mass. These background levels have to be subtracted from the measured signals to obtain the correct mixing ratios in the air sample. In PTR-MS, the background levels are determined by diverting the sample flow through a catalytic converter using two three-way valves (see Fig. 1). The converter consists of a stainless steel chamber with Pt-coated quartz wool (Shimadzu) heated to 350 °C, which efficiently removes the VOCs from the sample. The key motivation for using a catalytic converter is that it does not remove water vapor from the sample, as opposed to other filter materials such as activated charcoal. This is important because the background impurities may depend on the humidity of the sampled air. Moreover, the proton-transfer reactions in the PTR-MS can be influenced by the humidity, as will be seen in the next section.

A number of air samples were analyzed using a combination of gas chromatography (GC) and PTR-MS. This allows the different VOCs that are detected at the same mass, to be separated based on their different retention times in the GC column. In the setup used in Innsbruck, described by Fall et al. [19], the volatiles in ambient air were collected in Tenax adsorption tubes. The adsorption tubes were thermally desorbed in the laboratory prior to injection

onto the GC column (J&W scientific fused silica, DB 1701). The helium carrier gas in the column ($1 \text{ STP cm}^3 \text{ min}^{-1}$) was diluted in a flow of synthetic air ($9 \text{ STP cm}^3 \text{ min}^{-1}$) prior to the analysis by the PTR-MS. In the setup developed in Utrecht, samples were collected in Tedlar bags and pre-concentrated in a cold trap slightly above the temperature of liquid nitrogen. The trap was heated to 100 °C and volatiles were injected onto the GC column (Varian fused silica, CP Sil 5CB). The helium carrier gas ($3 \text{ STP cm}^3 \text{ min}^{-1}$) was diluted in synthetic air ($50\text{--}100 \text{ STP cm}^3 \text{ min}^{-1}$) before the analysis by PTR-MS. A flame-ionization detector (FID) was used in parallel to the PTR-MS for an independent measurement of the hydrocarbons in the He carrier gas.

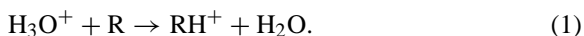
3. Sensitivity

The sensitivity of PTR-MS depends on many different factors, including (1) the current of H_3O^+ ions from the ion source, (2) the extent of the reaction between H_3O^+ ions and VOCs in the drift tube, and (3) the collection and detection efficiency of reagent and product ions by the quadrupole mass spectrometer. In this section, we will focus on point (2), the reactions of H_3O^+ in the drift tube, as it is important to understand this part of the setup in detail, and also because it gives some flexibility to optimize the operating conditions for specific compounds. For instance, the conversion efficiency of primary into product ions is increased at a higher pressure in the drift tube. However, at a constant electric field, this means that the ion kinetic energy is reduced and that cluster ions become more prevalent, in which case their reactions with the VOCs of interest need to be taken into account. On the other hand, a reduced ion kinetic energy may also reduce the degree of fragmentation of product ions, which can be advantageous for some compounds.

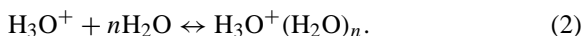
3.1. Ion-molecule reactions in the PTR-MS

In PTR-MS, proton-transfer reactions with H_3O^+ ions are used to ionize the organic trace gases R in the

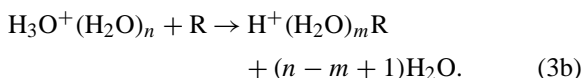
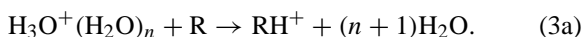
sampled air:



These reactions are exothermic if the proton affinity (PA) of R is higher than the PA of water (166.5 kcal mol⁻¹), in which case the reaction proceeds at a rate close to the collision rate of a few times 10⁻⁹ cm³ molecule⁻¹ s⁻¹ [28]. In addition to reaction (1), the H₃O⁺ (and RH⁺) ions can cluster with water molecules in the sampled air:



These cluster ions would be a problem because their presence complicates the interpretation of the mass spectra. In PTR-MS, cluster ion formation is effectively prevented by increasing the average kinetic energy of the ions using an electric field over the entire length of the drift tube. Depending on the electric field and pressure in the drift tube, however, H₃O⁺(H₂O)_n cluster ions can be present in the drift tube and react by:



Since the proton affinities of (H₂O)_n water clusters are higher than that of H₂O, the proton-transfer reaction (3a) is more selective than reaction (1): some trace gases R do react with H₃O⁺ but not with H₃O⁺(H₂O)_n ions. The rate of the ligand-switching reaction (3b) depends on the dipole moment of R: for polar molecules ligand switching can be as efficient as proton transfer, whereas for non-polar compounds such as benzene, reaction (3b) does not occur. The cluster ions formed by reaction (3b) are in most cases less strongly bound than the H₃O⁺(H₂O)_n clusters, which means that they will dissociate in the drift tube leading to formation of RH⁺ and RH⁺(H₂O). Depending on the operating conditions both reactions (3a) and (3b) can therefore lead to formation of RH⁺ ions, but since the cluster ion distribution may depend on the concentration of water vapor in the drift tube, the detection efficiency can be humidity dependent [27].

3.2. Distribution of cluster ions in the drift tube

As a result of the electric field *E* in the drift tube, the ions obtain an increased velocity, the so-called drift velocity *v_d*, given by [29]:

$$v_d = \mu \times E, \quad (4)$$

where μ is the ion mobility. The ion mobility has been determined for numerous ions in different buffer gases, including for H₃O⁺ ions in nitrogen [30,31]. Generally, the reduced mobility μ_0 is reported:

$$\mu_0 = \left(\frac{p}{p_0}\right) \left(\frac{T_0}{T}\right) \times \mu = \left(\frac{N}{N_0}\right) \times \mu. \quad (5)$$

In this equation, *p* is the pressure, *T* the temperature and *N* the number density of the gas in the drift tube. The parameter *N₀* is the gas number density at standard pressure *p₀* (1 atm) and temperature *T₀* (273.15 K). Substituting Eq. (5) into (4) gives:

$$v_d = \mu_0 N_0 \times \left(\frac{E}{N}\right). \quad (6)$$

This shows that the drift velocity is a function of the parameter *E/N*, which is frequently used in ion mobility studies and is expressed in units of Townsend (1 Td = 10⁻¹⁷ V cm²).

The temperature of the ions is higher than the drift-tube temperature *T* as a result of the selective heating of the ions by the electric field. The average center-of-mass kinetic energy of collisions between ions and neutrals in a buffer gas ⟨KE_{cm}⟩, is given by the Wannier expression [32]:

$$\langle \text{KE}_{\text{cm}} \rangle = \frac{(m_i + m_b)m_n}{2(m_i + m_n)} v_d^2 + \frac{3}{2} k_B T = \frac{3}{2} k_B T_{\text{coll}}, \quad (7)$$

where *m_i*, *m_b* and *m_n* are the masses of the reagent ion, the buffer gas and the neutral, respectively, *k_B* is Boltzmann's constant and *T_{coll}* is the temperature associated with ⟨KE_{cm}⟩. According to Eq. (7) the ion temperature *T_{coll}* is different for every neutral species in the drift tube. For collisions with the buffer gas itself (in this case air) *m_n* = *m_b* and Eq. (7) reduces to:

$$\langle \text{KE}_{\text{cm}} \rangle_{\text{buffer}} = \frac{1}{2} m_b v_d^2 + \frac{3}{2} k_B T = \frac{3}{2} k_B T_{\text{eff}}. \quad (8)$$

For a limited number of cases it has been shown that the effective temperature T_{eff} describes the internal energy of the ion reactants [32] and it is used, therefore, in this work to describe the temperature of the H_3O^+ ions and the degree of clustering with water molecules in the drift tube. From Eqs. (6) and (8) it can be seen that T_{eff} depends only on E/N .

Lau et al. [33] measured the equilibrium constants for the association and dissociation reactions (2) as a function of the temperature. Assuming that the effect of the electric field can be described by an enhanced ion temperature equal to T_{eff} , the distribution of $\text{H}_3\text{O}^+(\text{H}_2\text{O})_n$ cluster ions in the drift tube can be calculated depending on the parameter E/N and the concentration of water in the drift tube. Results are shown in Fig. 2 and were calculated for dry sample air. A small fraction (5%) of the water vapor flowing through the ion source reaches the drift tube [27], which causes the formation of the clusters in Fig. 2. It can be seen that the overall cluster size decreases with increasing E/N until all ions are converted into H_3O^+ at approximately 120 Td.

Measurements of the cluster ion distribution may give significantly different results from the calculated

distribution, for example due to collision-induced dissociation of the water cluster ions in the intermediate chamber between the drift tube and quadrupole chamber. Included in Fig. 2 are the measured fractions of H_3O^+ (circles) and $\text{H}_3\text{O}^+(\text{H}_2\text{O})$ ions (diamonds) and they can be seen to be in reasonable agreement with the calculation. In this experiment, the potentials in the intermediate chamber were chosen such that collision-induced dissociation was kept at a minimum. The agreement is in general much worse at lower E/N values. Warneke et al. [27] found indirect evidence that the calculated cluster ion distributions are reasonable by measuring the drift velocity of ions in the drift tube. Recently, detailed studies by Hanson indicate that Eq. (8) may be an overestimate of the temperature [34], possibly due to the fact that the association reactions are better described by the lower T_{coll} than by T_{eff} .

The effect of humidity on the cluster ion distribution is demonstrated in Fig. 3, which shows the fraction of H_3O^+ ions in the drift tube as a function of the partial water pressure in the sampled air. The range spans from 0 to 40 mbar, which is equivalent to a relative humidity range of 0–100% at an air temperature of 30 °C. At an E/N of 120 Td, the effect of humidity is very minor. At 100 Td, the fraction of H_3O^+ ions is

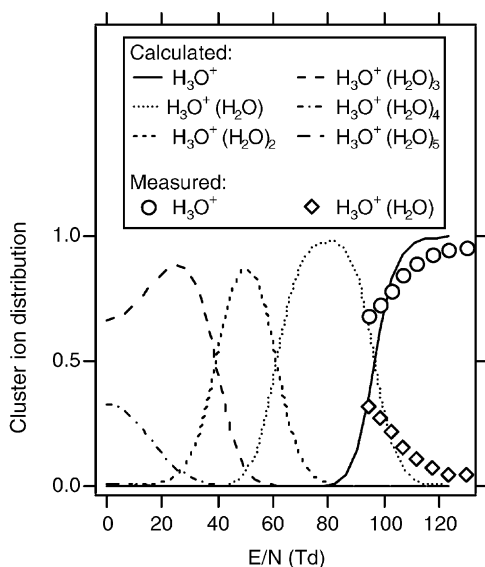


Fig. 2. Distribution of $\text{H}_3\text{O}^+(\text{H}_2\text{O})_n$ cluster ions in the drift tube of a PTR-MS instrument as a function of the parameter E/N .

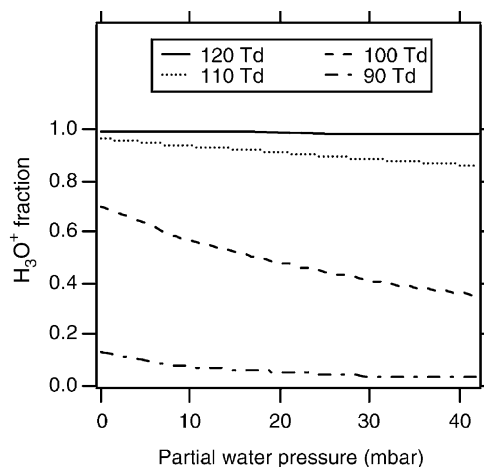


Fig. 3. The effect of the humidity of the sampled air on the $\text{H}_3\text{O}^+(\text{H}_2\text{O})_n$ cluster ion distribution in the drift tube of the PTR-MS. The curves show the number of H_3O^+ ions as fraction of the total for four different values of the parameter E/N .

strongly dependent on the humidity, whereas at 90 Td, most of the reagent ions are cluster ions.

3.3. Sensitivity of PTR–MS

The density of H_3O^+ ions after traversing the drift tube with the reaction time Δt can be described as

$$[\text{H}_3\text{O}^+]_{\Delta t} = [\text{H}_3\text{O}^+]_0 \exp(-k[\text{R}]\Delta t). \quad (9)$$

In this equation, $[\text{H}_3\text{O}^+]_0$ is the density of reagent ions injected from the ion source, k is the rate coefficient for the proton-transfer reaction (1), and $[\text{R}]$ is the concentration of trace gas R. It is assumed that the only loss of reagent ions occurs through reaction (1). In reality, the radial diffusion of ions and collisions with the wall of the drift tube leads to additional losses. It can be shown, however, that such losses are relatively small in the PTR–MS under the operating conditions that are normally used. Also, in Eq. (9) it is assumed that there is only one trace gas R reacting with H_3O^+ . If there are more, as in any air sample, the term $k[\text{R}]\Delta t$ in Eq. (9) has to be replaced with $\sum k_i[\text{R}_i]\Delta t$, where the summation is made over all the different trace gases present. The density of RH^+ ions produced from reaction (1) is given by

$$\begin{aligned} [\text{RH}^+] &= [\text{H}_3\text{O}^+]_0 \{1 - \exp(-k[\text{R}]\Delta t)\} \\ &\approx [\text{H}_3\text{O}^+]_0 k[\text{R}]\Delta t. \end{aligned} \quad (10)$$

The approximation in Eq. (10) is justified if $k[\text{R}]\Delta t$ is small, in other words if only a small fraction of H_3O^+ ions reacts in the drift tube. Eq. (10) shows that under these conditions the density of RH^+ ions at the end of the drift tube is proportional to the concentration of the trace gas R. If $[\text{R}]$ is too high, then the approximation in Eq. (10) is no longer justified and the production of RH^+ ions is non-linear in $[\text{R}]$, which should be avoided.

The reaction time Δt is determined by the ion drift velocity and the length L of the drift tube (9.6 cm). Warneke et al. [27] measured the drift velocity of ions in the drift tube of the PTR–MS, and found that the velocity is the same for all the $\text{H}_3\text{O}^+(\text{H}_2\text{O})_n$ cluster ions. This may come as a surprise, since these cluster

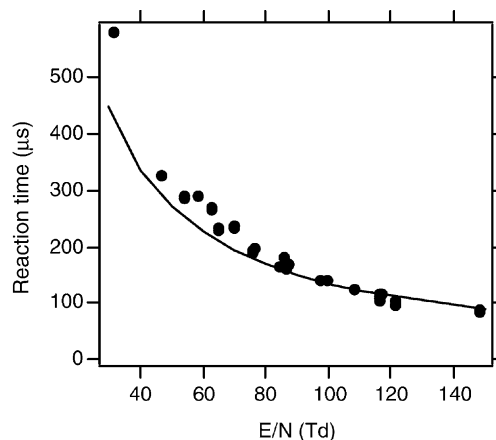


Fig. 4. Residence time of ions in the drift tube. The solid circles are measurement results, whereas the full curve is calculated using Eq. (11).

ions have different ion mobilities, but merely reflects the fact that the association and dissociation reactions (2) are in equilibrium: the number of ligands attached to an individual ion changes many times during its residence time in the drift tube. Fig. 4 shows a comparison between the reaction time measured by Warneke et al. [27], and the reaction time calculated from the drift velocity v_d (Eq. (7)):

$$\Delta t = \frac{L}{\mu_0 N_0} \times \left(\frac{E}{N}\right)^{-1}. \quad (11)$$

The full curve was calculated using the reduced mobility of H_3O^+ ($2.76 \text{ cm}^2 \text{ V}^{-1} \text{ s}^{-1}$). Therefore, the agreement between the measured and calculated reaction times is good for E/N above 100 Td, where H_3O^+ is indeed the most abundant ion in the drift tube (see Fig. 2). At lower E/N values, the higher $\text{H}_3\text{O}^+(\text{H}_2\text{O})_n$ clusters dominate. These have lower mobilities, and hence the calculation according to Eq. (11) underestimates the measured reaction time.

Using Eqs. (10) and (11), the fraction of H_3O^+ ions that is converted into RH^+ ions can be expressed as

$$\begin{aligned} \frac{[\text{RH}^+]}{[\text{H}_3\text{O}^+]_0} &= [\text{R}] \times \frac{kL}{\mu_0 N_0} \times \left(\frac{E}{N}\right)^{-1} \\ &= \text{VMR} \times \frac{kL}{\mu_0 N_0} \times \frac{N^2}{E}, \end{aligned} \quad (12)$$

where VMR is the volume mixing ratio of trace gas R. From Eq. (12) we can obtain the sensitivity, defined as the signal of RH^+ ions obtained at a VMR of 1 ppbv and normalized to a H_3O^+ signal of $10^6 \text{ counts s}^{-1}$:

$$\text{Sensitivity} = 10^{-3} \times \frac{kL}{\mu_0 N_0} \times \frac{N^2}{E} \times \frac{T(\text{RH}^+)}{T(\text{H}_3\text{O}^+)}. \quad (13)$$

The sensitivity is expressed in units of normalized counts $\text{s}^{-1} \text{ ppbv}^{-1}$ (ncps ppbv^{-1}). In Eq. (13) the factors $T(\text{RH}^+)$ and $T(\text{H}_3\text{O}^+)$ are the detection efficiencies for RH^+ and H_3O^+ ions, respectively. The differences in these factors are determined by the mass-dependent transmission of the mass filter and to a lesser extent by the electrostatic lenses, which focus the ions onto the quadrupole entrance. The ratio $T(\text{RH}^+)/T(\text{H}_3\text{O}^+)$ has to be determined experimentally, for instance by adding a single compound R and by measuring the decrease in the H_3O^+ signal simultaneously with the increase in RH^+ signal.

Fig. 5 shows a comparison between the sensitivity for acetonitrile calculated using Eq. (13) and the sensi-

tivity measured using a calibrated mixture of acetonitrile (and several other VOCs) in nitrogen. A reaction rate coefficient of $k = 3.0 \times 10^{-9} \text{ cm}^3 \text{ molecule}^{-1} \text{ s}^{-1}$ was used in the calculation, measured for the enhanced kinetic energy in the drift tube, and the transmission factor $T(\text{RH}^+)/T(\text{H}_3\text{O}^+)$ was measured to be 1.6. Eq. (13) shows that the sensitivity is dependent on the pressure squared (Fig. 5a): both the reaction time and the frequency of reactions between H_3O^+ and trace molecules depend linearly on the pressure. However, at a constant value of E/N , the sensitivity depends linearly on the pressure (Fig. 5b): only the reaction frequency is varied. Both curves agree reasonably well with the measurements, shown by the open circles in Fig. 5. Reasons for the discrepancies may include (1) the dependence of the transmission factor on the pressure in the drift tube, and (2) the dependence of the proton-transfer reaction on the kinetic energy, which is not a constant in the measurement at constant electric field. Although the agreement between calculation and measurement in Fig. 5 shows that the rate of the proton-transfer reactions in the drift tube is reasonably well understood, the remaining discrepancies indicate the importance of calibrating the sensitivity of PTR-MS rather than using calculated calibration factors.

From Eq. (13) it is clear that the sensitivity can be improved by increasing the pressure and the length of the drift tube. In practice, the pressure in the PTR-MS is limited by the pumping speeds of the system. Moreover, operating the system at a higher pressure means that the electric field must also be increased in order to operate at the same E/N value. A discharge of the electric field over the length of the drift tube starts to become possible at higher fields and pressures. Increasing the length means that the potential of the ion source has to be multiplied by a similar factor, which may be difficult to achieve in practice.

3.4. Reverse proton-transfer reactions

If the proton affinity (PA) of a compound R is only slightly higher than the PA of water, then the reverse

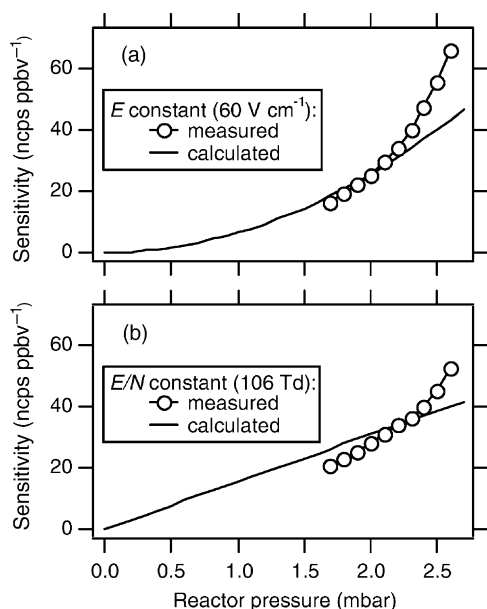
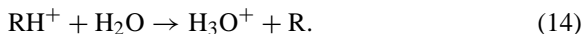


Fig. 5. Measured and calculated sensitivity of PTR-MS for acetonitrile as a function of the pressure at (a) a constant electric field of 60 V cm^{-1} , and (b) a constant E/N value of 106 Td .

of reaction (1) starts to play a role in PTR–MS:



As reaction (14) is endothermic, the rate coefficient is much smaller than for the forward reaction (1). However, the concentration of water in the drift tube is much larger than the concentration of R, and therefore, the forward and backward reactions may be of similar importance. Moreover, the ion kinetic energy is elevated in the PTR–MS, and endothermic reactions are thus more important than based solely on the reaction enthalpy. The backward reaction (14) was shown to be significant in the case of formaldehyde (HCHO ; $\text{PA} = 171.7 \text{ kcal mol}^{-1}$) [35]. As a consequence, the sensitivity of PTR–MS for formaldehyde is significantly smaller compared with other VOCs, and moreover strongly dependent on the humidity. Similar problems are expected for the detection of hydrogen sulfide (H_2S) and hydrogen cyanide (HCN). Recently, Hanson has shown that as a result of this effect the sensitivity at higher drift tube pressures can become slightly humidity dependent even for methanol (CH_3OH ; $\text{PA} = 181.9 \text{ kcal mol}^{-1}$) [34], as opposed to the results shown by Warneke et al. [27], which were obtained at lower pressure.

4. Specificity

4.1. Urban air (city of Utrecht)

In Fig. 6 chromatograms are presented, which were obtained using a GC–PTR–MS analysis of an urban air sample. The sample was collected from the roof of the Buys Ballot laboratory, a seven-story building in Utrecht, The Netherlands. The laboratory is close to the city of Utrecht and next to a major highway, and hence the air samples were heavily influenced by car emissions. Over the course of this work, several tens of samples were analyzed, which showed, of course, differences in the mixing ratios, but the chromatograms observed for these samples were essentially no different from those shown here. The PTR–MS instrument was operated at a

drift tube pressure of 2.3 mbar and an E/N value of 106 Td.

Also shown in the bottom panel of Fig. 6 is the FID signal, which was recorded simultaneously. At retention times longer than 35 min, the background starts to increase significantly and also a number of peaks are present which are due to the Tedlar bag that was used to store the air samples.

4.2. Remote air (Sonnblick Observatory in the Austrian Alps)

In Fig. 7 chromatograms are presented, obtained using a GC–PTR–MS analysis of air samples collected at the Sonnblick Observatory. The Sonnblick is a 3106 m (a.s.l.) high mountain within the central ridge of the Austrian Alps, located about 150 km southeast of Munich, Germany, and 100 km south of Salzburg, Austria. Due to the high altitude, this site usually allows sampling of free tropospheric air. Karl et al. [18] and Fall et al. [19] described the conditions during these measurements in detail and presented some results that are complementary to the chromatograms shown in Fig. 7. The sampling period was about 10 days following the detection of large diurnal peaks of biogenic VOCs at this high-altitude site. Nevertheless, biogenic VOC mixing ratios in the hundreds of pptv range were still detectable during sampling.

The drift tube in the Innsbruck PTR–MS was operated at 2 mbar and an E/N value of 140 Td. As compared with the Utrecht PTR–MS, these conditions give a somewhat lower conversion efficiency of primary into product ions. The increased kinetic energy effectively eliminates the presence of any cluster ions, but can also lead to more fragmentation of the product ions. An example of this is shown below for ethyl benzene, which fragments at 140 Td but not at 106 Td.

4.3. Discussion

4.3.1. Methanol

Methanol (CH_3OH ; 32 amu) is a ubiquitous compound in the atmosphere. Even in remote conditions, background levels of around 1 ppbv are observed, as a

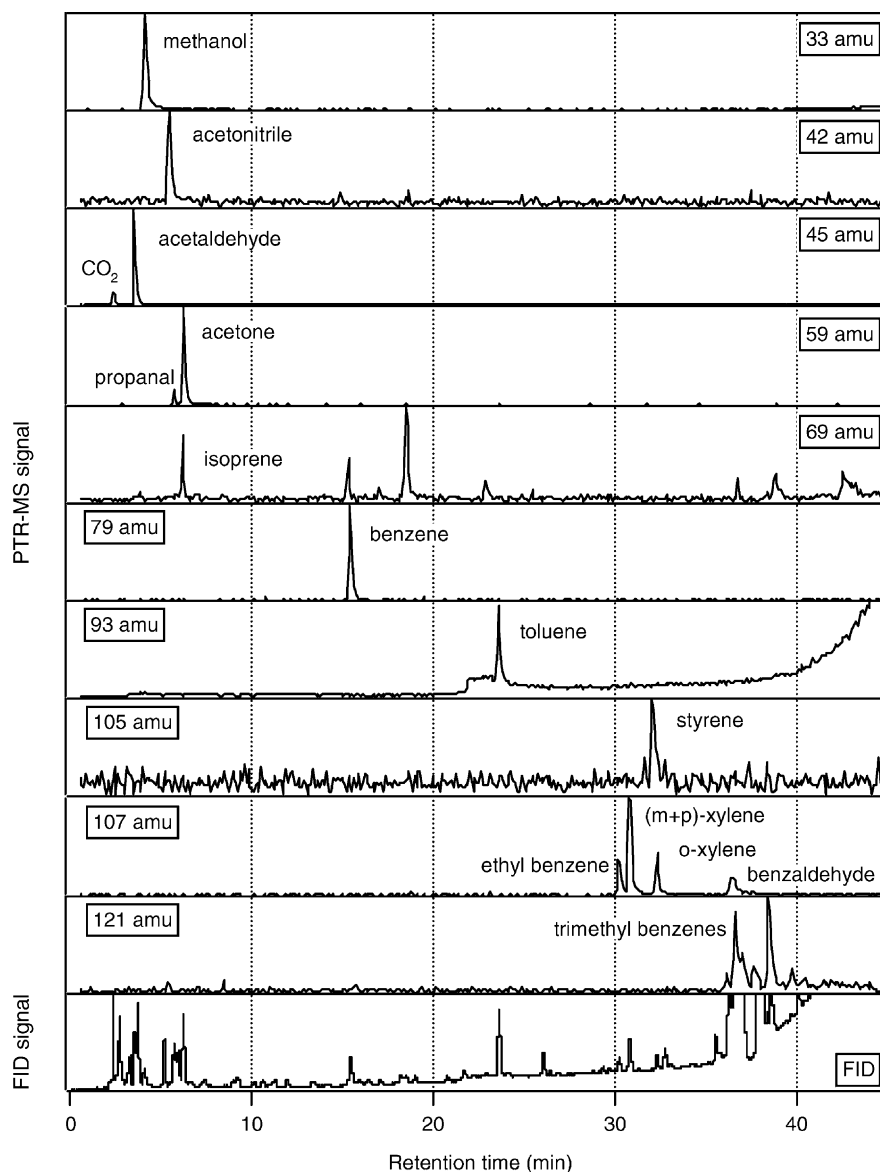


Fig. 6. Chromatograms resulting from a GC–PTR–MS and GC–FID analysis of an urban air sample collected in Utrecht.

result of large sources from vegetation and a relatively long atmospheric lifetime [36].

The chromatograms measured at 33 amu (the mass of protonated methanol) of both the urban air (Fig. 6) and the Sonnblick samples (Fig. 7) only contain one peak, corresponding to methanol. We believe therefore that PTR–MS measurements of methanol in the atmo-

sphere are most likely not influenced by interference from other compounds. This conclusion is supported by isotope measurements of de Gouw et al. [25], who demonstrated that in a laboratory study of plant emissions, the signal at mass 34 amu was about 1.1% of that at mass 33 amu, indicating that the compound detected at these masses has one carbon atom.

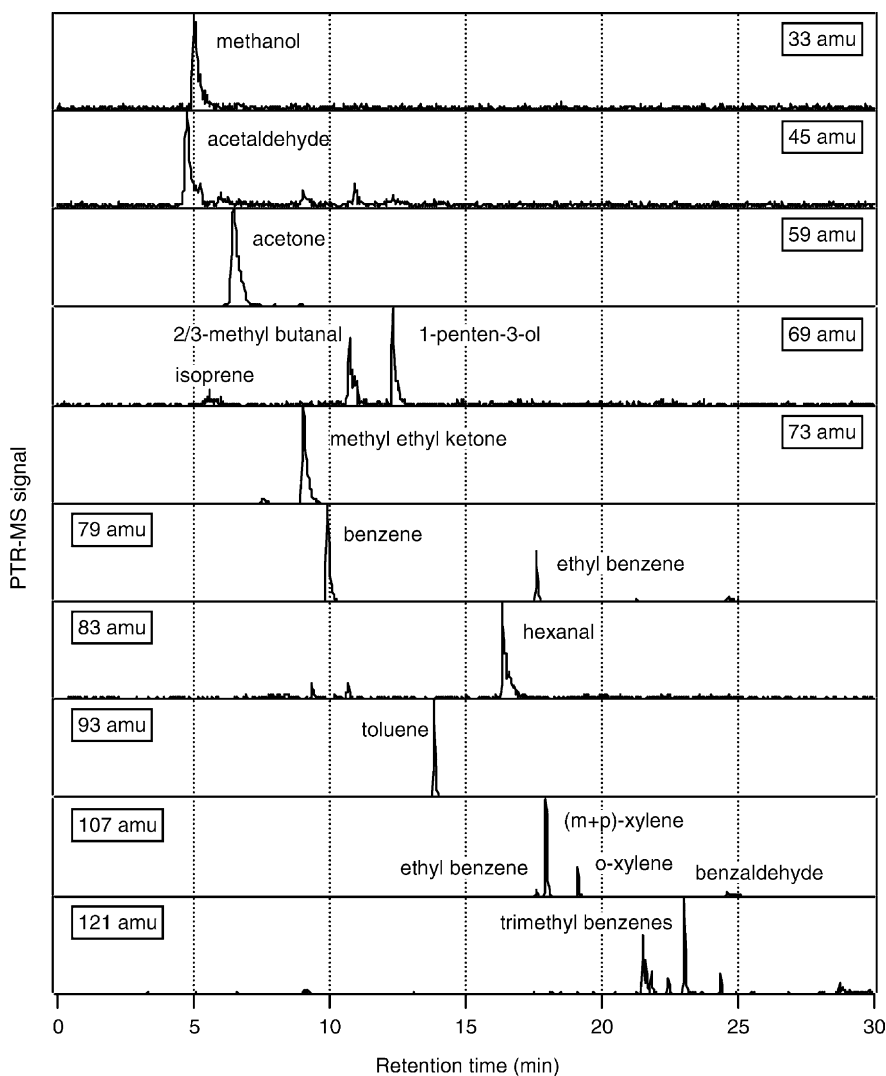


Fig. 7. Chromatograms resulting from a GC–PTR–MS analysis of an air sample collected at the Sonnblick Observatory.

4.3.2. Acetonitrile

Acetonitrile (CH_3CN ; 41 amu) is a common compound in the atmosphere, and is observed even in remote conditions at mixing ratios of 100–150 pptv. Its main source is believed to be the burning and smoldering of biomass and bio-fuels. The lifetime against the reaction with hydroxyl radicals is long (1 year), but ocean uptake has been suggested to be a more efficient loss process [37]. Its behavior in the

atmosphere is in many respects very similar to that of hydrogen cyanide (HCN) [38].

Fig. 6 shows that the only peak in the chromatogram measured at mass 42 amu is attributed to acetonitrile. We believe therefore that PTR–MS measurements of acetonitrile are most likely not influenced by interference from other compounds. Further evidence was collected during a brief inter-comparison performed in Utrecht, the results of which are shown in Fig. 8. The

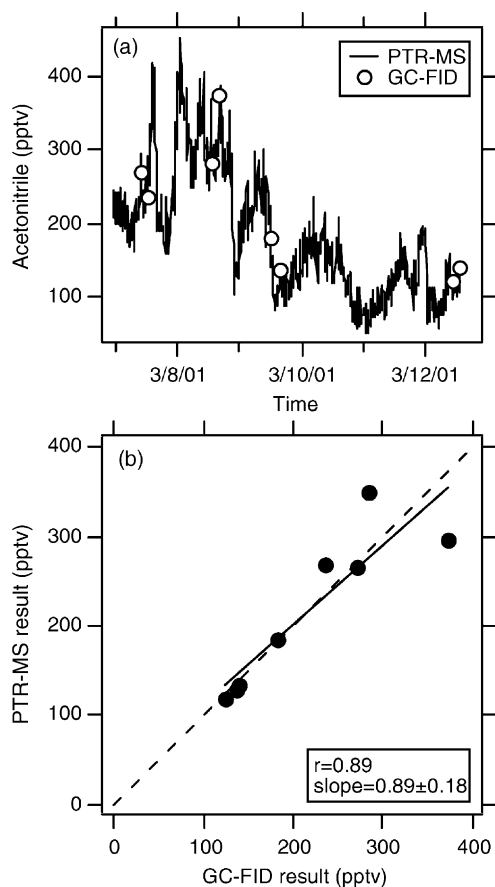


Fig. 8. Inter-comparison between measurements of acetonitrile (CH_3CN) using PTR-MS and GC-FID. Panel (a) shows both measurement results vs. time. Panel (b) shows the correlation between the two results. The solid circles are the measurement results, the full line shows the result of a linear fit to the data, and the dashed line is the one-to-one relationship.

mixing ratio of acetonitrile was monitored during several days using PTR-MS. The results were compared to those of GC-FID analyses of a number of samples collected in Tedlar bags during this period. It can be seen from Fig. 8 that the agreement between the two independent measurements is reasonable (linear correlation coefficient $r = 0.89$). The two data points that are furthest away from the one-to-one relationship, indicated by the dashed line, are taken during the period on March 8 when the mixing ratio was highly variable, which may explain some of the discrepancy.

4.3.3. Acetaldehyde

Acetaldehyde (CH_3CHO ; 44 amu) is a common photo-oxidation product of many organic compounds in the atmosphere. It is a reactive compound itself and an efficient precursor of peroxyacetyl nitrate (PAN; $\text{CH}_3\text{C}(\text{O})\text{OONO}_2$) in polluted air, which is an important reservoir species for nitrogen oxides (NO_x). Reliable acetaldehyde measurements are valuable to help constrain the models that describe organic carbon chemistry in the atmosphere.

Figs. 6 and 7 show chromatograms measured at mass 45 amu of samples collected in Utrecht and at the Sonnblick. In this case, there is a difference between the two chromatograms. Apart from the main peak due to acetaldehyde, the chromatogram in Fig. 6 shows a peak at a very short retention time, which we attribute to carbon dioxide (CO_2). Because CO_2 is not adsorbed on Tenax, it is clear why this peak does not show up in the Sonnblick sample. Using calibrated mixtures of CO_2 in air we found that the signal at 45 amu is weakly dependent on CO_2 (approximately $0.4 \text{ counts s}^{-1} \text{ ppmv}^{-1}$). A possible explanation is the formation of CO_2H^+ ions in the intermediate chamber between the drift tube and the quadrupole MS chamber. In principle, the contribution of CO_2 to the signal at mass 45 does not interfere with the measurement of acetaldehyde at this mass: the catalytic converter which is used to remove acetaldehyde and to determine the background level in the system, does not remove CO_2 and its contribution to the signal is thus properly accounted for. Interference from CO_2 to the signal at mass 45 amu can only be a problem in conditions where (1) CO_2 is highly variable and (2) acetaldehyde mixing ratios are low, but this is very rarely the case.

The sample collected in Utrecht does not show any peaks besides acetaldehyde and CO_2 , whereas in the Sonnblick sample a few minor peaks are visible at longer retention times. This is surprising given the fact that an urban air sample is likely to contain more compounds at higher mixing ratios. There seem to be two alternative explanations. First, the Sonnblick samples were collected on Tenax, which is not very efficient in adsorbing the small hydrocarbons. The relative peak

heights in Fig. 7 can therefore be misleading. Second, the PTR–MS in Utrecht was used at a lower ion kinetic energy than the instrument in Innsbruck, which reduces the fragmentation of product ions as mentioned before. It is possible that the small peaks in the Sonnblick sample are due to compounds, which do not fragment to mass 45 in the Utrecht instrument. In summary, it cannot be ruled out entirely that PTR–MS measurements of acetaldehyde suffer from minor interference by other compounds, perhaps depending on the operating conditions. Although it seems likely that the measurement of acetaldehyde by PTR–MS is free from interference, more research is necessary to study these details.

4.3.4. Acetone

Acetone (CH_3COCH_3 ; 58 amu) is an omnipresent compound in the atmosphere. It can be formed in the atmosphere from oxidation of propane, monoterpenes, etc., and has also direct sources in biomass burning and vegetation [36]. The scientific interest in atmospheric acetone has been intensified by the work of Singh et al. [39] who demonstrated that this compound might play an important role as a source of hydroxyl radicals in the upper troposphere.

Figs. 6 and 7 both contain a chromatogram measured at mass 59 amu. It is interesting to note that the Sonnblick sample only shows a peak due to acetone, whereas the sample from Utrecht shows two peaks attributed to acetone and propanal ($\text{C}_2\text{H}_5\text{CHO}$; 58 amu). It is clear that acetone and propanal cannot be separated using PTR–MS. Propanal, however, has a much shorter atmospheric lifetime than acetone (9 h vs. 5 weeks), which may explain why it is observed in the urban air sample from Utrecht and not in the more remote location on top of the Sonnblick. In most of the chromatograms observed over the course of this work, propanal was only a small fraction of the mixing ratio of acetone. In air masses that are not recently impacted by fresh emission sources, it is likely that propanal mixing ratios are low and that the measurement of acetone by PTR–MS is free from interference. On the other hand, the atmospheric chemistry of propanal is not well understood suggesting that

acetone measurements should be regarded with some caution.

4.3.5. Isoprene

Approximately, 450 Tg per year of isoprene ($\text{CH}_2=\text{C}(\text{CH}_3)\text{CH}=\text{CH}_2$; 68 amu) is released to the atmosphere by forest trees and other vegetation. Combined with its high reactivity, this means that isoprene is one of the most important VOCs to consider in the chemistry of the troposphere [40].

Both chromatograms in Figs. 6 and 7 show several peaks measured at 69 amu, including a contribution from isoprene. It is clear that in these conditions the PTR–MS measurement at mass 69 is not a reliable indicator of isoprene mixing ratios. The samples in Utrecht were collected in the late winter in a city, whereas the sample from the Sonnblick was collected in the fall in a region where biogenic emissions are dominated by other compounds. This explains the low levels of isoprene in the two air samples. From the measurements it is clear that there are a number of compounds that can interfere with the measurement of isoprene by PTR–MS.

High mixing ratios of isoprene were inferred from aircraft measurements using PTR–MS over the rainforest in Surinam, and a reasonable correlation was found between the PTR–MS data and the results obtained from GC–FID analyses of air samples collected during the flights [14]. However, in conditions where the GC results indicated near-zero isoprene mixing ratios, the PTR–MS still detected a few hundred pptv for this compound. A possible explanation could be the interference from compounds such as present in the chromatograms in Figs. 6 and 7. In the vicinity of strong isoprene emitters, the PTR–MS measurements of this compound are likely free from significant interference by other compounds. In other air masses, however, care must be taken in interpreting the results.

4.3.6. Methyl ethyl ketone

There have only been a limited number of measurements of methyl ethyl ketone (MEK) or butanone ($\text{C}_2\text{H}_5\text{COCH}_3$; 72 amu) in the atmosphere. MEK is expected to have sources in the atmosphere from

photo-oxidation of butane and higher hydrocarbons. Work by Kirstine et al. [41] and de Gouw et al. [25] has shown that vegetation can be a direct source.

The chromatogram in Fig. 7 measured at 73 amu only shows one peak, which is attributed to MEK. Similar to acetone, however, one can expect interference from butanal ($\text{C}_3\text{H}_7\text{CHO}$; 72 amu). More work is necessary to determine the specificity of MEK measurements by PTR–MS. Measurements at 73 amu can suffer from a relatively high background level of ions due to the formation of $\text{H}_3\text{O}^+(\text{H}_2\text{O})_3$ ions in the drift tube. The background level depends on the humidity of the sampled air, but also on the operating conditions: at higher E/N the background levels are lower. These factors must be carefully considered when trying to quantify MEK in ambient air.

4.3.7. Aromatic compounds

Aromatic compounds are common in air masses impacted by urban and industrial pollution and are among the most efficient precursors for ozone and organic aerosol formation in the atmosphere [42,43]. The ability of PTR–MS to measure these compounds can therefore contribute to regional air quality studies.

Warneke et al. [27] performed an inter-comparison between PTR–MS and GC–FID measurements of benzene (C_6H_6 ; 78 amu) and toluene ($\text{C}_6\text{H}_5\text{CH}_3$; 92 amu). The agreement between the two measurements was satisfactory, but it was also found that the sensitivity can be dependent on the humidity at lower E/N values. The chromatograms shown in Fig. 6 measured at masses 79 and 93 amu show the presence of only benzene and toluene at their respective masses. The chromatogram at mass 93 amu shows an enhanced background at longer retention times due to impurities in the column, which was relatively new at the time these measurements were done. The chromatogram in Fig. 7 at mass 93 amu only shows a peak due to toluene. There is therefore ample evidence that PTR–MS measurements of toluene are free from interference by other compounds. The chromatogram in Fig. 7 at mass 79 amu, however, shows a peak attributed to ethyl benzene apart from the main peak due to benzene. The finding that ethyl benzene is partly

detected at mass 79 amu in the Sonnblick samples but not in the sample from Utrecht is easily explained by the higher ion kinetic energy used in the Sonnblick measurements, and agrees with recent laboratory studies by Midey et al. [44]. It demonstrates that PTR–MS measurements of benzene, if performed under the appropriate operating conditions, are likely free from interference. This involves operating the PTR–MS at a lower value of the parameter E/N , in which case the humidity dependence of the sensitivity needs to be carefully considered.

Fig. 6 contains a chromatogram measured at mass 105 amu. The chromatogram shows only one peak due to styrene ($\text{C}_6\text{H}_5\text{CH=CH}_2$; 104 amu), a highly reactive aromatic hydrocarbon, which is emitted in small quantities from cars. An inter-comparison between PTR–MS and GC–FID measurements of styrene is presented in Fig. 9. The mixing ratio of styrene was monitored from the roof of the laboratory in Utrecht during several days using PTR–MS. The results were compared to those of GC–FID analyses of a number of samples collected in Tedlar bags during this period. It is seen from Fig. 9 that the correlation between the two results is reasonable ($r = 0.88$), but that the absolute value of the mixing ratios is somewhat different. This may be due to the fact that the response factor of both the PTR–MS and the GC–FID were only estimated in this case, or to an incorrectly determined background of around 40 pptv in the PTR–MS measurements. Nevertheless, these results suggest that PTR–MS measurements of styrene may be free from interference by other compounds.

Figs. 6 and 7 contain two chromatograms measured at mass 107 amu. In both samples, the chromatogram shows contributions from ethyl benzene, three xylene isomers and benzaldehyde. These compounds all have the same mass (106 amu) and cannot be separated using PTR–MS. Also, the compounds have similar sources (emissions from automobiles) and atmospheric lifetimes (1–2 days), and it is therefore expected that in most air masses a PTR–MS measurement at mass 107 amu contains contributions from all these compounds. An experiment was done to find out if a PTR–MS measurement at mass 107 amu can

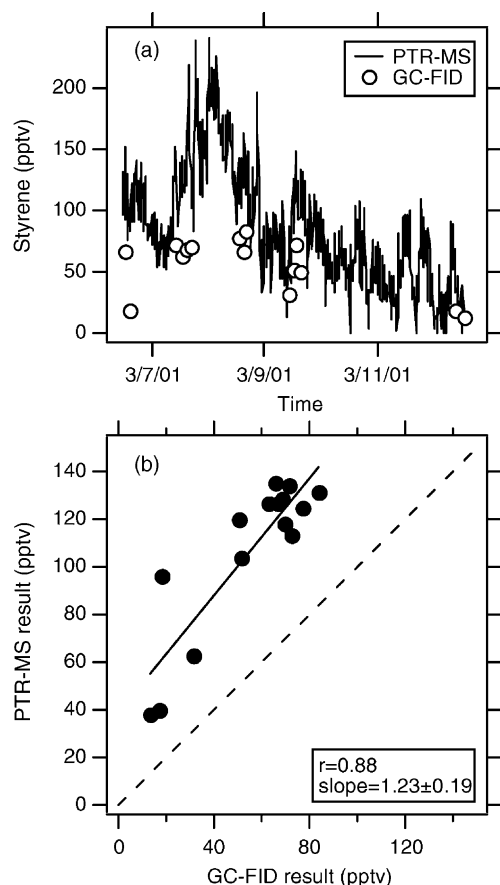


Fig. 9. Inter-comparison between measurements of styrene using PTR-MS and GC-FID measurements. Panel (a) shows the results of both measurements vs. time. Panel (b) shows the correlation between the two results.

be regarded as the sum of the mixing ratios of ethyl benzene, the three xylene isomers and benzaldehyde. The signal at 107 amu was monitored over a number of days from the top of the laboratory in Utrecht and the result is shown in Fig. 10a, along with the results of GC-FID analyses of a number of samples collected in Tedlar bags during this period. The contribution from benzaldehyde could not be determined from the GC-FID measurements, because the peak co-elutes with the trimethyl benzenes (see Fig. 6). The sum of the GC-FID data on ethyl benzene and xylene is compared with the on-line PTR-MS measurements in Fig. 10a and b (solid symbols) and it can be seen that

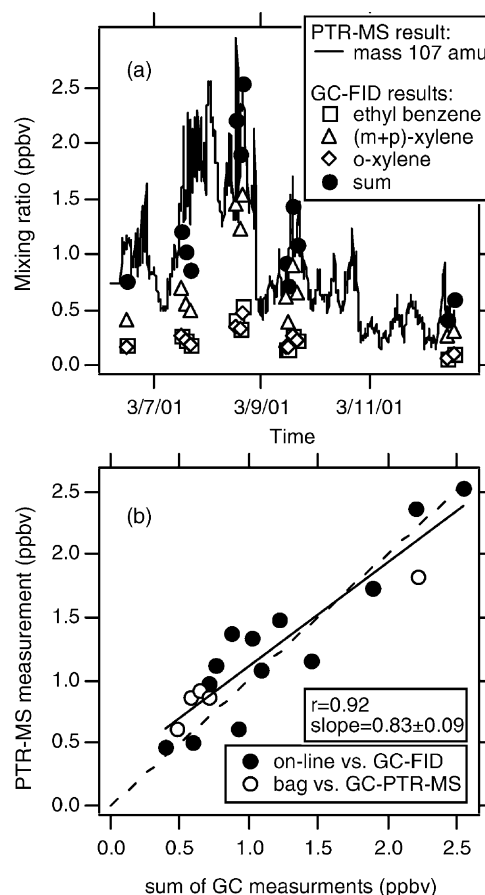


Fig. 10. Inter-comparison between PTR-MS measurements at mass 107 amu and GC measurements of ethyl benzene, xylene and benzaldehyde. Panel (a) shows the measurements vs. time. Panel (b) shows the correlation. The solid circles show the correlation between the on-line PTR-MS and GC-FID measurements from panel (a). The open circles show the correlation between direct PTR-MS vs. GC-PTR-MS measurements of other bag samples (see text).

the agreement is satisfactory, despite the fact that the contribution from benzaldehyde was not considered. After this period, another set of Tedlar bag samples was collected and analyzed by PTR-MS, GC-FID and GC-PTR-MS. From the latter analyses, the mixing ratio of benzaldehyde could be determined. Included in Fig. 10b is the comparison between the PTR-MS results and the sum of the GC-PTR-MS measurements of ethyl benzene, the xylenes and benzaldehyde

(open circles). Again, the agreement is satisfactory, and we conclude that the signal recorded by PTR–MS at 107 amu can likely be regarded as the sum of the mixing ratios of ethyl benzene, the three xylene isomers and benzaldehyde.

The chromatograms at mass 121 amu (Figs. 6 and 7) contain peaks attributed to different trimethyl benzenes, ethyl methyl benzenes, propyl benzene, and possibly other compounds (e.g., tolualdehydes). More work is necessary to find out if a PTR–MS measurement at 121 amu can be regarded as a sum measurement of the C₃-benzenes, as in the case of the previously discussed C₂-benzenes.

The samples in Utrecht were collected near a major highway, and the observed mixing ratios exhibited therefore a profile characteristic for emissions from traffic. In Fig. 11, the measured distribution of the different aromatic compounds is compared with the emission profiles for road transport used in CORINAIR (CORE Inventory AIR emissions) [45], which has been developed for the European Environment Agency. The open bars in Fig. 11 show the measured distribution of aromatic hydrocarbons, as a fraction of the total. The measurement results were obtained from a number of different samples, and the error bars in Fig. 11 show

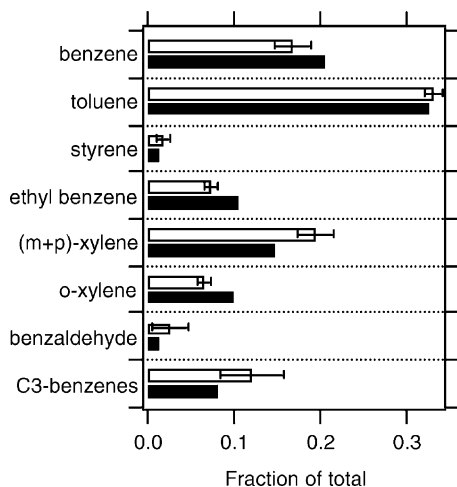


Fig. 11. Distribution of aromatic hydrocarbons measured in Utrecht (open bars) compared with the emission profile for gasoline cars with three-way catalytic converters (solid bars).

the standard deviation. The measurements are compared with the emission profiles for gasoline-powered vehicles with three-way catalysts, and it can be seen that the agreement is good. This further improves our confidence of the reliability of aromatic hydrocarbon measurements by PTR–MS.

4.3.8. Other compounds

Other VOCs that have been detected with PTR–MS are briefly mentioned here. Dimethyl sulfide or DMS (CH_3SCH_3) is emitted from phytoplankton in the ocean, and may be the most important natural sulfur compound in the atmosphere [46]. During a recent experiment performed on a platform in the North Sea, we compared PTR–MS measurements of DMS at mass 63 amu with GC measurements, and a preliminary analysis suggests that the agreement is good.

The concentrations of isoprene oxidation products, such as methyl vinyl ketone (MVK), methacrolein (MACR), and possibly isoprene hydro-peroxides, were inferred from PTR–MS measurements onboard a Citation research aircraft flying over a rainforest in Surinam [14]. The signals for masses 71 and 101 were used for the sum of MVK and MACR and isoprene hydro-peroxides, respectively. Although these identifications were not independently verified, there was good correlation at times with expected isoprene chemistry. More recently, another airborne PTR–MS instrument was used to measure isoprene and its oxidation products over oak forest sources in eastern Texas. In this case there was confirmation by simultaneous fast GC–FID analyses that masses 69 and 71 are highly correlated with isoprene and MVK + MACR, respectively [47].

Karl et al. [18] reported on PTR–MS measurements of atmospheric VOCs that can also be produced by vegetation when the leaves are damaged by freeze-thaw treatment [19]. GC–PTR–MS analyses demonstrated that a variety of C₅ and C₆ VOCs are formed by this treatment, presumably by well-known leaf wound pathways [24,48]. This work also revealed the complexity of biogenic C₅ VOCs that exhibit mass 69 during PTR–MS analyses, including for example isoprene, methylbutanals, and pentenols. These

findings emphasize the need for GC analyses to verify the identity of VOCs detected by PTR–MS.

5. Conclusion

Proton-transfer-reaction mass spectrometry has emerged as a useful tool for studying the atmospheric chemistry of volatile organic compounds. PTR–MS allows measurements of many important VOCs both from natural and man-made origins, plus their atmospheric oxidation products. The compact design and fast response time facilitate the use of the method in measurements even from aircraft.

In this paper, it is shown how the sensitivity and selectivity of PTR–MS depend on the operating conditions of the instrument. It is shown how the sensitivity can be optimized and the role played by the humidity of the sample gas is studied.

Gas chromatographic separation was used in combination with PTR–MS to analyze a number of samples from the Sonnblick Observatory in Austria and from the city of Utrecht in The Netherlands. GC–PTR–MS proved to be a highly useful tool to investigate possible interference in the PTR–MS measurements. The results shown here are promising as they suggest that PTR–MS measurements of many compounds are free from interference. In addition, for other compounds we are beginning to understand which different compounds may contribute to the signal at their respective masses.

Acknowledgements

We thank David Hanson for useful discussions, Arnaud Kok for performing the ion velocity measurements, and Willem Kegel for making a GC available for this work. Carsten Warneke acknowledges financial support from FOM and NWO. This work was also supported by the Austrian Fonds zur Förderung der wissenschaftlichen Forschung (Project 14130), and by NSF grant ATM-9805191 (to R.F.). T.K. was also supported by the Advanced Study Program and the

Atmospheric Chemistry Program, National Center for Atmospheric Research.

References

- [1] C.N. Hewitt (Ed.), *Reactive Hydrocarbons in the Atmosphere*, Academic Press, San Diego, 1999.
- [2] B.J. Finlayson-Pitts, J.N. Pitts Jr., *Science* 276 (1997) 1045.
- [3] W. Lindinger, A. Hansel, A. Jordan, *Int. J. Mass Spectrom. Ion Process.* 173 (1998) 191.
- [4] L.G. Huey, E.J. Dunlea, E.R. Lovejoy, D.R. Hanson, R.B. Norton, F.C. Fehsenfeld, C.J. Howard, *J. Geophys. Res.* 103 (1998) 3355.
- [5] T.M. Miller, J.O. Ballenthin, R.F. Meads, D.E. Hunton, W.F. Thorn, A.A. Viggiano, Y. Kondo, M. Koike, Y. Zhao, *J. Geophys. Res.* 105 (2000) 3701.
- [6] R.L. Mauldin III, D.J. Tanner, J.A. Heath, B.J. Huebert, F.L. Eisele, *J. Geophys. Res.* 104 (1999) 5801.
- [7] D.J. Tanner, A. Jefferson, F.L. Eisele, *J. Geophys. Res.* 102 (1997) 6415.
- [8] J. Schneider, V. Bürger, F. Arnold, *J. Geophys. Res.* 102 (1997) 25501.
- [9] H. Berresheim, J.W. Huey, R.P. Thorn, F.L. Eisele, D.J. Tanner, A. Jefferson, *J. Geophys. Res.* 103 (1998) 1629.
- [10] T. Reiner, O. Möhler, F. Arnold, *J. Geophys. Res.* 104 (1999) 13943.
- [11] P.J. Crutzen, et al., *Atmos. Environ.* 34 (2000) 1161.
- [12] U. Pöschl, J. Williams, P. Hoor, H. Fischer, P.J. Crutzen, C. Warneke, R. Holzinger, A. Hansel, A. Jordan, W. Lindinger, H.A. Scheeren, W. Peters, J. Lelieveld, *J. Atmos. Chem.* 38 (2001) 115.
- [13] J. Williams, U. Pöschl, P.J. Crutzen, A. Hansel, R. Holzinger, C. Warneke, W. Lindinger, J. Lelieveld, *J. Atmos. Chem.* 38 (2001) 133.
- [14] C. Warneke, R. Holzinger, A. Hansel, A. Jordan, W. Lindinger, U. Pöschl, J. Williams, P. Hoor, H. Fischer, P.J. Crutzen, H.A. Scheeren, J. Lelieveld, *J. Atmos. Chem.* 38 (2001) 167.
- [15] J.A. de Gouw, C. Warneke, H.A. Scheeren, C. van der Veen, M. Bolder, M.P. Scheele, J. Williams, S. Wong, L. Lange, H. Fischer, J. Lelieveld, *J. Geophys. Res.* 106 (2001) 28469.
- [16] J. Lelieveld, et al., *Science* 291 (2001) 1031.
- [17] C. Warneke, J.A. de Gouw, *Atmos. Environ.* 35 (2001) 5923.
- [18] T. Karl, R. Fall, P.J. Crutzen, A. Jordan, W. Lindinger, *Geophys. Res. Lett.* 28 (2001) 507.
- [19] R. Fall, T. Karl, A. Jordan, W. Lindinger, *Atmos. Environ.* 35 (2001) 3905.
- [20] T. Karl, A. Guenther, A. Jordan, R. Fall, W. Lindinger, *Atmos. Environ.* 35 (2001) 491.
- [21] H.J.I. Rinne, A.B. Guenther, C. Warneke, J.A. de Gouw, S.L. Luxembourg, *Geophys. Res. Lett.* 28 (2001) 3139.
- [22] R. Holzinger, C. Warneke, A. Hansel, A. Jordan, W. Lindinger, D.H. Scharffe, G. Schade, P.J. Crutzen, *Geophys. Res. Lett.* 26 (1999) 1161.

- [23] C. Warneke, T. Karl, H. Judmaier, A. Hansel, A. Jordan, W. Lindinger, P.J. Crutzen, *Global Biogeochem. Cycles* 13 (1999) 9.
- [24] R. Fall, T. Karl, A. Hansel, A. Jordan, W. Lindinger, J. *Geophys. Res.* 104 (1999) 15963.
- [25] J.A. de Gouw, C.J. Howard, T.G. Custer, R. Fall, *Geophys. Res. Lett.* 26 (1999) 811.
- [26] J.A. de Gouw, C.J. Howard, T.G. Custer, B. Baker, R. Fall, *Environ. Sci. Technol.* 34 (2000) 2640.
- [27] C. Warneke, C. van der Veen, S. Luxembourg, J.A. de Gouw, A. Kok, *Int. J. Mass Spectrom.* 207 (2001) 167.
- [28] K.F. Lim, J.I. Brauman, *J. Chem. Phys.* 94 (1991) 7164.
- [29] E.A. Mason, E.W. McDaniel, *Transport Properties of Ions in Gases*, Wiley, New York, 1988.
- [30] L.A. Viehland, E.A. Mason, *At. Data Nucl. Data Tables* 60 (1995) 37.
- [31] I. Dotan, D.L. Albritton, W. Lindinger, M. Pahl, *J. Chem. Phys.* 65 (1976) 5028.
- [32] A.A. Viggiano, R.A. Morris, *J. Phys. Chem.* 100 (1996) 19227.
- [33] Y.K. Lau, S. Ikuta, P. Kebarle, *J. Am. Chem. Soc.* 104 (1982) 1462.
- [34] D.R. Hanson, private communication.
- [35] A. Hansel, W. Singer, A. Wisthaler, M. Schwarzmann, W. Lindinger, *Int. J. mass Spectrom.* 167/168 (1997) 697.
- [36] H.B. Singh, Y. Chen, A. Tabazadeh, Y. Fukui, I. Bey, R. Yantosca, D. Jacob, F. Arnold, K. Wohlfrom, E. Atlas, F. Flocke, D. Blake, B. Heikes, J. Snow, R. Talbot, G. Gregory, G. Sachse, S. Vay, Y. Kondo, *J. Geophys. Res.* 105 (2000) 3795.
- [37] A.T.J. de Laat, J.A. de Gouw, A. Hansel, J. Lelieveld, *J. Geophys. Res.* 106 (2001) 28481.
- [38] Q. Li, D.J. Jacob, I. Bey, R.M. Yantosca, Y. Zhao, Y. Kondo, J. Notholt, *Geophys. Res. Lett.* (2000).
- [39] H.B. Singh, M. Kanakidou, P.J. Crutzen, D.J. Jacob, *Nature* 378 (1995) 50.
- [40] A.B. Guenther, et al., *J. Geophys. Res.* 100 (1995) 8873.
- [41] W. Kirstine, I. Galbally, Y. Ye, M. Hooper, *J. Geophys. Res.* 103 (1998) 10605.
- [42] R.G. Derwent, M.E. Jenkin, S.M. Saunders, M.J. Pilling, *Atmos. Environ.* 32 (1998) 2429.
- [43] J.R. Odum, T.P.W. Jungkamp, R.J. Griffin, R.C. Flagan, J.H. Seinfeld, *Science* 276 (1997) 96.
- [44] K.A.J. Midey, S. Williams, S.T. Arnold, R.A. Morris, A.A. Viggiano, *J. Chem. Phys.*, submitted for publication.
- [45] <http://www.aeat.co.uk/netcen/corinair/testnewlayout/homepage.html>.
- [46] R.J. Charlson, J.E. Lovelock, M.O. Andreae, S.G. Warren, *Nature* 326 (1987) 655.
- [47] P.G. Goldan, A. Hansel, private communication.
- [48] A.J. Fisher, A.J. Curtis, H.D. Grimes, R. Fall, *Plant Biol.*, submitted for publication.